MOLECULAR AND CELLULAR BIOLOGY, Dec. 1997, p. 7069–7076 Vol. 17, No. 12
0270-7306/97/$04.00+0

Base Pair Conformation-Dependent Excision of Benzo[*a*]Pyrene Diol Epoxide-Guanine Adducts by Human Nucleotide Excision Repair Enzymes

MARTIN T. HESS,[1] DANIELA GUNZ,[1]† NATALIA LUNEVA,[2] NICHOLAS E. GEACINTOV,[2] AND HANSPETER NAEGELI[1]*

Institute of Pharmacology and Toxicology, University of Zürich-Tierspital, 8057 Zürich, Switzerland,[1] and Chemistry Department, New York University, New York, New York 10003[2]

Received 17 June 1997/Returned for modification 30 July 1997/Accepted 8 September 1997

Human nucleotide excision repair processes carcinogen-DNA adducts at highly variable rates, even at adjacent sites along individual genes. Here, we identify conformational determinants of fast or slow repair by testing excision of N^2-guanine adducts formed by benzo[*a*]pyrene diol epoxide (BPDE), a potent and ubiquitous mutagen that induces mainly G · C→T · A transversions and frameshift deletions. We found that human nucleotide excision repair processes the predominant (+)-*trans*-BPDE-N^2-dG adduct 15 times less efficiently than a standard acetylaminofluorene-C^8-dG lesion in the same sequence. No difference was observed between (+)-*trans*- and (−)-*trans*-BPDE-N^2-dG, but excision was enhanced about 10-fold by changing the adduct configurations to either (+)-*cis*- or (−)-*cis*-BPDE-N^2-dG. Conversely, excision of (+)-*cis*- and (−)-*cis*- but not (+)-*trans*-BPDE-N^2-dG was reduced about 10-fold when the complementary cytosine was replaced by adenine, and excision of these BPDE lesions was essentially abolished when the complementary deoxyribonucleotide was missing. Thus, a set of chemically identical BPDE adducts yielded a greater-than-100-fold range of repair rates, demonstrating that nucleotide excision repair activity is entirely dictated by local DNA conformation. In particular, this unique comparison between structurally highly defined substrates shows that fast excision of BPDE-N^2-dG lesions is correlated with displacement of both the modified guanine and its partner base in the complementary strand from their normal intrahelical positions. The very slow excision of carcinogen-DNA adducts located opposite deletion sites reveals a cellular strategy that minimizes the fixation of frameshifts after mutagenic translesion synthesis.

Mammalian nucleotide excision repair promotes genomic stability by removing UV radiation products and a wide range of chemical carcinogen-DNA adducts (14, 20, 37, 42, 52). This multisubunit DNA repair system operates by cleavage of damaged strands on either side of the targeted lesion (28, 35) followed by excision of oligonucleotide segments 24 to 32 residues in length (25, 31). In subsequent reactions, double-helical integrity and the correct nucleotide sequence are reestablished by DNA repair synthesis and DNA ligation (1, 40).

The mechanism by which mammalian nucleotide excision repair enzymes discriminate damaged sites as substrates for dual DNA incision is not understood (14, 24, 26, 42), but several reports have demonstrated that excision activity is highly nonuniform in the context of mammalian chromosomes. For example, bulky UV radiation products are excised at variable rates, with cyclobutane pyrimidine dimers being processed considerably more slowly than the less frequently occurring pyrimidine(6-4)pyrimidone lesion (30). Generally, active genes are repaired faster than inactive loci, and the template strand of RNA polymerase II-transcribed genes is repaired faster than the coding strand (2, 3, 20, 29, 46). Yet another level of heterogeneity emerged when DNA excision repair rates were compared between closely related genomic sites. Along the nontranscribed strand of the human hypoxanthine phosphoribosyltransferase gene, for example, excision repair of guanine adducts formed by benzo[*a*]pyrene diol epoxide (BPDE) varies by more than 1 order of magnitude (48). Excision of 1-nitrosopyrene-induced guanine adducts in exactly the same region of the hypoxanthine phosphoribosyltransferase gene is also highly variable, but with a distinctly different pattern of site-specific repair (49). Similarly, in the *p53* and phosphoglycerate kinase 1 genes of UV-irradiated human fibroblasts repair rates of cyclobutane pyrimidine dimers vary dramatically with nucleotide position (16, 44). In the nontranscribed strand of *p53*, some sites are repaired with up to 90% efficiency within 24 h after irradiation whereas other positions along the same strand are less than 5% repaired in this time (44). Frequently, sites that are slowly repaired coincide with hot spots of BPDE- or UV-induced mutations (44, 48), indicating that the carcinogenesis process may be enhanced by inefficient repair of critical oncogene or tumor suppressor sequences.

Because of the molecular and clinical consequences of differential site-specific repair, it is essential to gain an understanding of the structural factors that determine the rate of excision in response to a particular DNA lesion. In this study, we exploited stereoisomeric BPDE-N^2-dG lesions, for which the conformational properties have been established in detail, to identify molecular determinants of human excision repair efficiency. Benzo[*a*]pyrene is a prototype carcinogen that is widely distributed in our environment and is metabolically activated to several genotoxic BPDE derivatives (5). As indicated in Fig. 1, racemic *anti*-BPDE generates mainly (+)-*trans*-BPDE-N^2-dG adducts with a minor proportion of (+)-*cis*-, (−)-*trans*-, and (−)-*cis*-BPDE-N^2-dG isomers (4). Depending on their stereochemistry, these lesions impose distinctly different structural alterations on DNA. Of the four stereoisomeric

* Corresponding author. Mailing address: Institute of Pharmacology and Toxicology, Winterthurerstrasse 260, 8057 Zürich, Switzerland. Phone: 41-1-635-8763. Fax: 41-1-635-8910.

† Present address: Imperial Cancer Research Fund, Herts, ENG 3LD, United Kingdom.

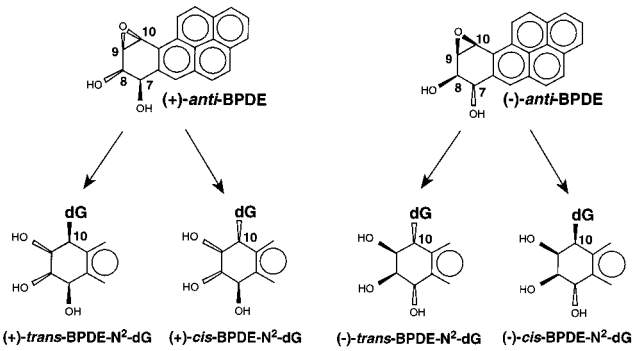

FIG. 1. Stereoisomeric N^2-guanine adducts formed by racemic *anti*-BPDE. Covalent addition of this ultimate carcinogen to guanine generates mainly (+)-*trans*-BPDE-N^2-dG with quantitatively minor (+)-*cis*-, (−)-*trans*-, and (−)-*cis*-BPDE-N^2-dG adducts. The (+) and (−) notations indicate mirror image relationships between the configurations of hydroxyl groups at the C-7, C-8, and C-9 chiral carbon centers. *Trans* and *cis* denote the configuration of covalent bonds between N^2 of guanine and carbon C-10 of the benzo[*a*]pyrenyl moiety.

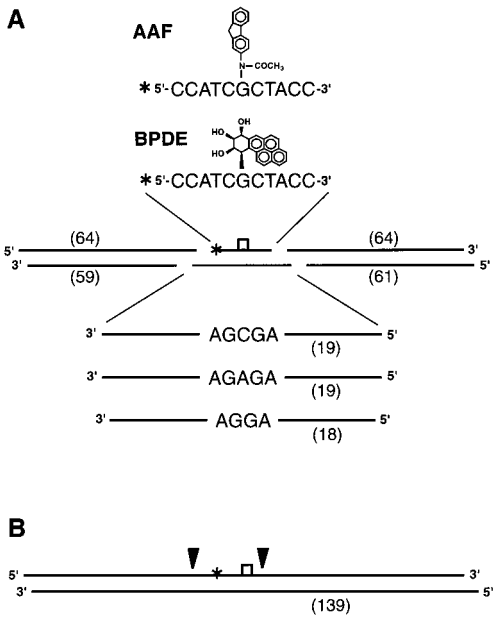

FIG. 2. Schematic representation of the oligonucleotide excision assay. (A) Internally labeled duplexes of 139 bp were assembled from six different oligonucleotides (their lengths are shown in parentheses). Modified 11-mer oligonucleotides (5′-CCATCGCTACC-3′) were prepared and characterized as outlined in Materials and Methods and contained an acetylaminofluorene (AAF) or a stereoselective BPDE adduct at the single guanine residue. Control substrates were constructed with unmodified 11-mers. Prior to ligation, the central 11-mer oligonucleotide was 5′ end labeled with [^{32}P]ATP (indicated by the asterisk) whereas the other five components were phosphorylated with nonradioactive ATP. Different complementary oligomers 19 or 18 nucleotides in length were used to either replace or delete the cytosine residue opposite the modified guanine. (B) After ligation and electrophoretic purification, the resulting 139-mer duplex substrate contained an internal radiolabel near the site-directed modification. The arrowheads indicate the expected major sites of dual DNA incision by human nucleotide excision repair. Typically, this endonucleolytic cleavage reaction generates a ladder of radiolabeled excision products in the range of 24 to 32 nucleotides in length.

BPDE-N^2-dG adducts, only (+)-*trans*-BPDE-N^2-dG is associated with strong DNA bending (53, 55). Furthermore, (+)-*trans*-BPDE-N^2-dG is more effective in causing DNA unwinding than the adducts derived from (−)-*anti*-BPDE (54). In the 5′-TCGCT-3′ sequence context used in the present study, nuclear magnetic resonance (NMR) analysis showed that (+)-*trans*- and (−)-*trans*-BPDE-N^2-dG adopt external adduct conformations that accommodate the benzo[*a*]pyrenyl moiety into the minor groove and retain Watson-Crick alignment at all bases (7, 12). In contrast, (+)-*cis*- and (−)-*cis*-BPDE-N^2-dG in the same 5′-TCGCT-3′ sequence adopt internal adduct conformations characterized by benzo[*a*]pyrenyl insertion into the double helix and concomitant disruption of Watson-Crick hydrogen bonding. As a consequence, these helix-inserted (+)-*cis* and (−)-*cis* configurations cause displacement of the covalently modified guanine and its cytosine partner into the major or minor groove (8, 11).

By altering substrate stereochemistry or deoxyribonucleotide composition, we found that human nucleotide excision repair processes a series of conformationally distinct BPDE-N^2-dG adducts with an over-100-fold range of different excision rates. In particular, (+)-*cis*- and (−)-*cis*-BPDE-N^2-dG adducts (as well as acetylaminofluorene-C^8-dG in the same sequence) were excised about 10-fold more effectively than the corresponding (+)-*trans*- and (−)-*trans*-BPDE-N^2-dG isomers. In addition, excision of BPDE-N^2-dG adducts was strongly modulated when the cytosine opposite to the lesion in the complementary strand was either replaced by another base or was missing entirely, as in mutagenic postreplication duplexes resulting from the insertion of adenine or the formation of frameshift deletions across the lesion. Collectively, these results reveal that efficient excision repair activity is correlated with BPDE-N^2-dG-induced base displacements that affect both strands of modified DNA. The present report also indicates that human DNA excision repair enzymes are able to discriminate against substrates containing deoxyribonucleotide deletions opposite carcinogen-DNA adducts, thereby avoiding the fixation of potentially deleterious frameshift mutations during the subsequent synthesis of excision repair patches.

MATERIALS AND METHODS

Oligonucleotide modification. BPDE-N^2-dG adducts were obtained by reacting racemic (±)-7β,8α-dihydroxy-9α,10α-epoxy-7,8,9,10-tetrahydro-benzo[*a*]pyrene (*anti*-BPDE) with the 11-mer oligonucleotide 5′-CCATCGCTACC-3′ as described previously (6, 17). The four stereospecific products were separated by preparative reversed-phase high-performance liquid chromatography (HPLC) on an octyldecyl silane Hypersil column (6, 17). To establish the purity and stereochemical identity of each HPLC fraction, the samples were subjected to enzyme digestion studies with snake venom phosphodiesterase and bacterial alkaline phosphatase and analysis by UV absorption and circular dichroism as reported previously (6, 7). A site-directed acetylaminofluorene-C^8-dG adduct was produced by incubating the 5′-CCATCGCTACC-3′ oligonucleotide with *N*-acetoxy-2-acetylaminofluorene (purchased from the National Cancer Institute Chemical Carcinogen Reference Standard Repository) as outlined previously (21). The resulting acetylaminofluorene-modified oligonucleotide migrated on a 20% polyacrylamide gel markedly more slowly than the unmodified control.

Excision repair substrates. Internally radiolabeled DNA duplexes of 139 bp were obtained by ligating an unmodified or modified 11-mer (5′-CCATCGCTA CC-3′) with five other partially overlapping oligonucleotides (Fig. 2) as previously described (23, 28). The sequence of the complementary 19-mer oligonucleotide was 5′-GCTCGGTAGCGATGGTCAG-3′. Alternatively, this 19-mer sequence was replaced by 5′-GCTCGGTAGAGATGGTCAG-3′ or 5′-GCTCG GTAGGATGGTCAG-3′ to obtain substrates containing a G · A mismatch or a deletion site, respectively (Fig. 2). The four flanking oligonucleotides of 59 to 64 residues had exactly the same sequences as those described by Matsunaga et al. (28). For construction of linear double-stranded substrates, the 11-mer (70 pmol) was 5′ end labeled with [γ-^{32}P]ATP (7,000 Ci/mmol; ICN Pharmaceuticals, Inc.) and mixed with 100 pmol of each of the other five oligonucleotides that were phosphorylated with cold ATP. The mixture was annealed in 40-μl reaction mixtures containing 50 mM Tris-HCl (pH 7.9), 100 mM NaCl, 1 mM dithiothreitol, and 10 mM $MgCl_2$. After being heated to 85°C for 2 min, the samples were cooled to room temperature and ligation was carried out for 18 h at 16°C in the presence of 1 mM ATP, 5 U of T4 DNA ligase (Life Technologies, Inc.), and 50 μg of bovine serum albumin/ml. The full-length fragments of 139 nucleotides were isolated by electrophoresis in a preparative 6% polyacrylamide gel, performed under denaturing conditions. The purified 139-mers were then resus-

pended in 50 mM Tris-HCl (pH 7.9), 100 mM NaCl, and 10 mM $MgCl_2$, reannealed, and repurified by 6% preparative polyacrylamide gel electrophoresis under native conditions. The resulting substrates were stored in small aliquots at −80°C.

Human excision repair assay. HeLa cells (American Type Culture Collection, Rockville, Md.) were grown in RPMI 1640 supplemented with 7% fetal bovine serum (Life Technologies, Inc.). The human xeroderma pigmentosum complementation group A lymphoid cell line GM2250 (National Institute of General Medical Sciences Human Genetic Mutant Cell Repository, Camden, N.J.) was grown in RPMI 1640 in the presence of 15% fetal bovine serum. Cell extracts with typical protein concentrations of 10 to 15 mg/ml were prepared by cell lysis and ammonium sulfate precipitation according to previously published methods (27, 51). Excision reactions were adapted from the method of Huang et al. (26) and contained (in 25 μl) 35 mM HEPES-KOH (pH 7.9), 60 mM KCl, 40 mM NaCl, 5.6 mM $MgCl_2$, 2 mM ATP, 80 μM (each) dATP, dCTP, dGTP, and TTP, 0.8 mM dithiothreitol, 0.4 mM EDTA, 3.4% (vol/vol) glycerol, 5 μg of bovine serum albumin, 5 fmol (75,000 dpm) of radiolabeled DNA substrate, and 50 μg (in protein equivalents) of HeLa or lymphoid cell extract. In addition, coincubation reactions were performed in which radiolabeled substrate containing a site-directed (−)-*cis*-BPDE-N^2-dG adduct (5 fmol) was mixed with a three- or ninefold molar excess (15 and 45 fmol, respectively) of linear DNA fragments containing the (+)-cis-BPDE-dG lesion located opposite a deoxyribonucleotide deletion. Alternatively, 5 fmol of the radiolabeled substrate was combined with either 15 or 45 fmol of undamaged duplexes in the normal complementary sequence. After various incubation times at 30°C, reactions were stopped by the addition of sodium dodecyl sulfate to 0.3% (wt/vol) and proteinase K to 200 μg/ml, followed by proteinase K digestion for 15 min at 37°C. DNA was repurified by phenol-chloroform extraction, and excision repair products were resolved by electrophoresis in 10% polyacrylamide denaturing gels and visualized by autoradiography. The fraction of excised lesions was quantified by counting Cerenkov radiation in the gel slices containing 24- to 32-nucleotide-long excision products as well as in the respective gel slices containing full-length substrates (Beckman LS 6000LL liquid scintillation counter). Excision activity was expressed as the percentage of radioactivity migrating within the 24- to 32-mer oligonucleotide size range relative to the total amount of radioactivity in each lane. Control reactions containing undamaged substrates yielded background excision levels of approximately 0.05%. In parallel, the relative level of damage excision was confirmed by scanning densitometry of oligonucleotides in the 24- to 32-mer size range on appropriately exposed X-ray films (Molecular Dynamics computing densitometer with ImageQuant software). The two different quantification methods involving either Cerenkov radiation measurements or densitometric scanning yielded essentially identical results.

RESULTS

Oligonucleotide excision by human nucleotide excision repair enzymes. Nucleotide excision repair activity was determined by the oligonucleotide excision assay devised by Huang et al. (25, 26). This cell-free assay exploits the unique dual DNA incision pattern of human nucleotide excision repair and therefore provides high levels of sensitivity and specificity. Appropriate DNA substrates of 139 bp with a site-directed carcinogen adduct in the sequence 5′-TCGCT-3′ were constructed from six different oligomers as illustrated in Fig. 2A. Prior to ligation, the central 11-mer oligonucleotide was labeled with [γ-^{32}P]ATP at its 5′ end so that the resulting 139-mer duplex contained an internal radiolabel in the vicinity of the acetylaminofluorene-C^8-guanine or BPDE-N^2-guanine lesion (Fig. 2B). After purification, the double-stranded fragments were incubated with a nucleotide excision repair-proficient HeLa cell extract (27, 51) in the presence of ATP and all four deoxyribonucleoside triphosphates. Damage-specific dual DNA incision by human nucleotide excision repair generates radioactive products 24 to 32 nucleotides in length (25, 26, 31), which were resolved by denaturing gel electrophoresis and visualized by autoradiography.

In vitro repair reactions performed with linear 139-mer substrate containing a site-directed acetylaminofluorene-C^8-dG adduct yielded specific excision products that migrated in the polyacrylamide gel as an oligomeric ladder with dominant lengths ranging from 26 to 28 nucleotides (Fig. 3A, lane 6). Minor amounts of smaller fragments result from partial degradation of the main excision products in the cell extract (26). This characteristic oligonucleotide excision pattern was highly reproducible when independent preparations of acetylaminofluorene-modified substrate or HeLa cell extract were tested. Excision repair activity was quantified by counting Cerenkov radiation in the gel slices containing the excision products and

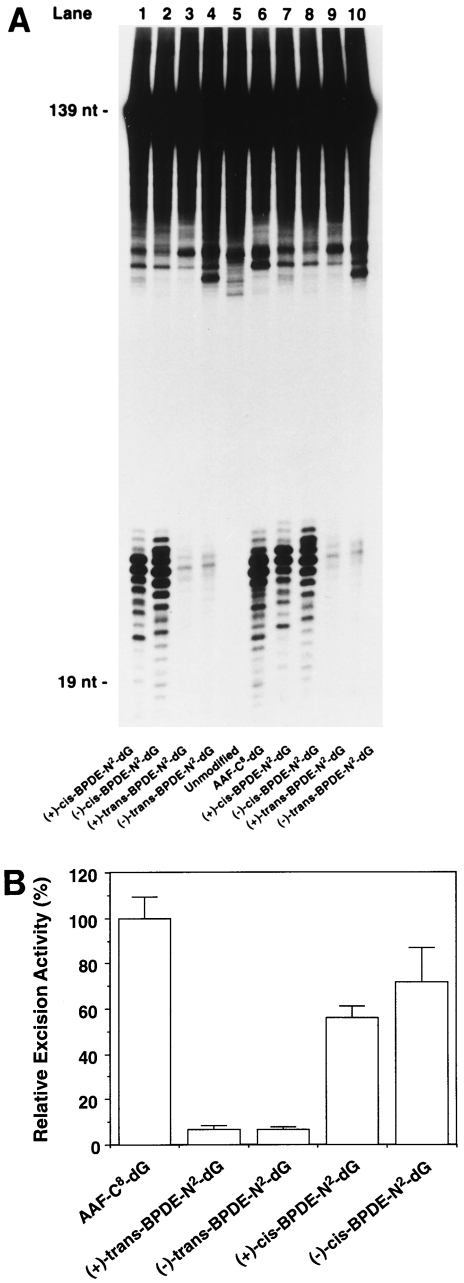

FIG. 3. Oligonucleotide excision by human nucleotide excision repair in response to acetylaminofluorene-C^8-guanine (AAF-C^8-dG) or stereospecific BPDE-N^2-dG adducts. The indicated linear substrates (5 fmol; 75,000 dpm per reaction) were incubated in HeLa cell extract for 40 min at 30°C. The reaction products were analyzed by polyacrylamide gel electrophoresis. (A) Representative gel visualized by autoradiography. The sizes of oligonucleotide excision products were estimated from a 19-mer marker; lane 5 shows a control reaction with unmodified substrate. nt, nucleotides. (B) Quantitative evaluation was performed by counting Cerenkov radiation and confirmed by laser scanning densitometry as outlined in Materials and Methods, and the relative excision repair activity is expressed as the percentage of oligonucleotide excision obtained in response to the AAF-C^8-guanine adduct (the bars show mean values of four to six independent experiments ± standard deviations).

full-length substrate, and these evaluations showed that 11.9% ± 1.2% of acetylaminofluorene adducts were excised during reaction times of 40 min. In contrast, no excision products were released from undamaged control substrate (Fig. 3A, lane 5), although intact 139-mer substrate as well as radioactive bands generated by nonspecific nuclease activity could be observed at similar levels at the top of the gel. This undamaged control demonstrates the absence of spurious DNA nicks or other lesions that may adversely affect the excision assay.

Excision of stereoisomeric BPDE-N^2-dG adducts. Homogeneous preparations of 11-mer primers containing one of four stereoselective BPDE-N^2-dG adducts were ligated into 139-mer duplexes as shown in Fig. 2 and incubated with HeLa cell extract. All four BPDE-N^2-dG stereoisomers were able to elicit human nucleotide excision repair activity, although at different rates. In particular, the representative polyacrylamide gel shown in Fig. 3A demonstrates that BPDE-N^2-dG adducts with *trans* configuration at the linkage sites were excised considerably more slowly than the corresponding stereoisomeric lesions with *cis* configuration (Fig. 3A, lanes 1 to 4 and 7 to 10, in duplicates). In all cases, the resulting excision products were in a size range similar to those induced by the acetylaminofluorene-C^8-guanine adduct (Fig. 3A, lane 6) and contained predominantly oligomeric components 26 to 30 nucleotides in length.

Nucleotide excision repair activity was quantified by counting Cerenkov radiation in the gel slices containing the excision products and the corresponding full-length substrates, and the relative levels of damage excision were additionally confirmed by laser scanning densitometry as indicated in Materials and Methods. These quantitative evaluations showed that (+)-*trans*-BPDE-N^2-dG was excised at a rate 15 times lower than that of the standard acetylaminofluorene-C^8-dG adduct in the same sequence context (Fig. 3B). A direct comparison between (+)-*trans*- and (−)-*trans*-BPDE-N^2-dG yielded identical excision rates (Fig. 3B), although these stereoisomeric BPDE adducts differ in the extent of DNA bending and unwinding (53–55) as well as in the orientation of their benzo[*a*]pyrenyl moiety within the minor groove (12). On the other hand, the carcinogen insertion and base displacement motif of (+)-*cis*- or (−)-*cis*-BPDE-N^2-dG (8, 11) was associated with an approximately 10-fold-higher excision rate relative to the Watson-Crick alignment characteristic of both (+)-*trans*- and (−)-*trans*-BPDE-N^2-dG (Fig. 3B). In the two *cis*-BPDE-N^2-dG adducts used in this study, the benzo[*a*]pyrenyl ring systems are oppositely oriented at their respective intercalation sites (11); in addition, the modified guanines are displaced into different grooves (11). However, these structural differences between the two *cis*-BPDE-N^2-dG variants seem to exert only minor effects on the overall excision efficiency (Fig. 3B).

Time course experiments confirmed that human nucleotide excision repair processes *trans*-BPDE-N^2-dG adducts with initial reaction rates that are about 1 order of magnitude lower than those stimulated by the corresponding *cis*-BPDE-N^2-dG isomers or the acetylaminofluorene-C^8-dG lesion (Fig. 4). Importantly, preferential excision of (+)-*cis*- and (−)-*cis*-BPDE-N^2-dG adducts relative to the *trans* isomers was highly reproducible when independent DNA substrate or human cell extract preparations were tested. In fact, the excision assays of Fig. 3, 4, and 5 were performed with different HeLa cell extract and substrate preparations. As expected, however, neither the *trans* nor the *cis* isomers of BPDE-N^2-dG were able to stimulate detectable excision reactions in nucleotide excision repair-deficient extracts from xeroderma pigmentosum complementation group A cells (gels not shown).

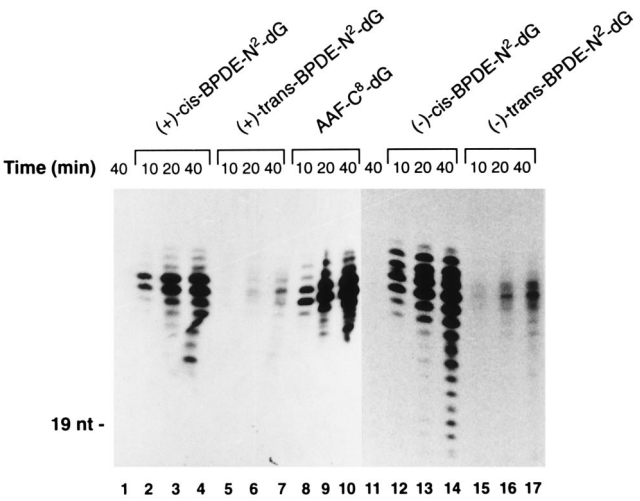

FIG. 4. Time course of oligonucleotide excision by human nucleotide excision repair. Incubations with HeLa cell extract were performed in the presence of linear DNA substrate (5 fmol; 75,000 dpm per reaction) containing one of the following adducts: (+)-*cis*-BPDE-N^2-dG adduct (lanes 2 to 4), (+)-*trans*-BPDE-N^2-dG (lanes 5 to 7), acetylaminofluorene-C^8-guanine (AAF-C^8-dG; lanes 8 to 10), (−)-*cis*-BPDE-N^2-dG (lanes 12 to 14), or (−)-*trans*-BPDE-N^2-dG (lanes 15 to 17). Repair incubations were stopped after 10, 20, or 40 min at 30°C and analyzed by polyacrylamide gel electrophoresis. The two autoradiographs were obtained simultaneously from parallel gels and with identical exposure times but with different cassettes. Only the bottom parts of the gels are shown; lanes 1 and 11 are control incubations of 40 min in the presence of undamaged substrate. nt, nucleotides.

Excision of BPDE-N^2-dG adducts with incorrect partner bases or deletion sites in the complementary strands. The dominant mutations induced by BPDE-N^2-dG lesions in mammalian cells involve G · C→T · A transversions (and thus the misincorporation of adenine opposite the covalently modified guanines during DNA replication) as well as frameshift deletions (33, 41, 47, 50). This pattern of mutagenesis prompted us to test excision repair of (+)-*trans*- and (+)-*cis*-BPDE-N^2-dG when the complementary cytosine was replaced by adenine. Similarly, we tested excision of the same BPDE-N^2-dG adducts when the deoxyribonucleotide residue opposite the modified guanines was missing. Appropriate linear DNA substrates containing (+)-*trans*- or (+)-*cis*-BPDE-N^2-dG lesions embedded in different sequence environments were prepared as depicted in Fig. 2. Human nucleotide excision repair activity in response to base alterations in the complementary undamaged strand was highly variable. Although all lanes in the polyacrylamide gel of Fig. 5A contained the same amount of total radioactivity, the tested substrates yielded very different excision repair activities. For example, excision of (+)-*trans*-BPDE-N^2-dG was marginally affected by the presence of adenine instead of cytosine in the partner strand (Fig. 5A, lanes 4 and 5). In contrast, excision repair of (+)-*cis*-BPDE-N^2-dG was markedly reduced when the complementary cytosine was replaced by adenine (Fig. 5A, lanes 7 and 8). Unexpectedly, excision repair of both (+)-*trans*- and (+)-*cis*-BPDE-N^2-dG was abolished following introduction of a deletion site opposite to the modified residue. In fact, no detectable oligonucleotide excision resulted from the incubations containing deletion duplexes either with a (+)-*trans*- (Fig. 5A, lane 6) or a (+)-*cis*-BPDE-N^2-dG lesion (Fig. 5A, lane 9). Appropriate control reactions established that the dG · dA mispair or the dC deletion site alone, i.e., in the absence of covalent BPDE-DNA modifications, fails to stimulate excision repair activity (Fig. 5A, lanes 2 and 3).

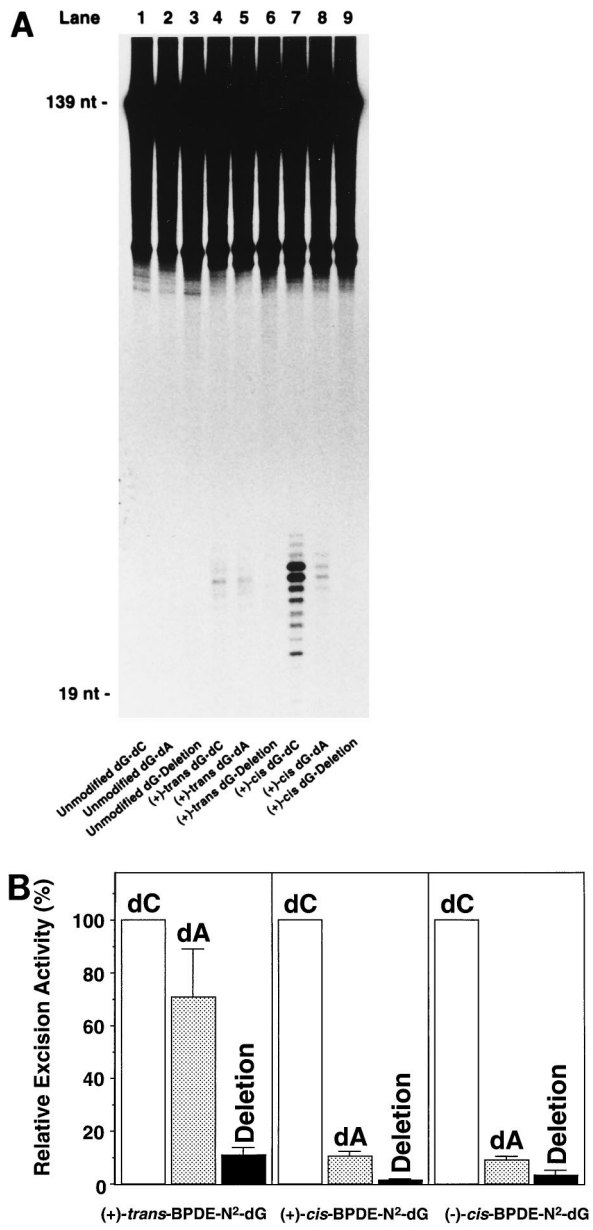

FIG. 5. Excision of (+)-*trans*-, (+)-*cis*-, and (−)-*cis*-BPDE-N^2-dG adducts opposite dC→dA replacement or dC deletion sites. Excision repair reactions were performed by incubating linear DNA substrate (5 fmol; 75,000 dpm per sample) in HeLa cell extract for 40 min at 30°C and were analyzed by polyacrylamide gel electrophoresis. Adduct conformation and the corresponding base composition of each substrate were as indicated. (A) Representative autoradiogram. No excision products were detected in control reactions incubated with unmodified substrate in the normal sequence (lane 1) or unmodified substrate containing either a dC→dA replacement (lane 2) or a single deletion site (lane 3). nt, nucleotides. (B) Quantitative evaluations were performed by counting Cerenkov radiation in the appropriate gel slices, and the results were confirmed by laser scanning densitometry as outlined in Materials and Methods; the relative excision repair activity is expressed as the percentage of oligonucleotide excision observed in response to either (+)-*trans*-, (+)-*cis*-, or (−)-*cis*-BPDE-N^2-dG in the fully complementary sequence, i.e., with dC opposite the lesion (the bars show mean values of three independent experiments ± standard deviations). The fractions of excised oligonucleotides in the control reactions with (+)-*trans*-, (+)-*cis*-, or (−)-*cis*-BPDE-N^2-dG opposite the regular cytosine residue were 0.9% ± 0.2%, 7.2% ± 1.1%, and 9.5% ± 2.2%, respectively.

Evaluation of several independent incubations by quantitative assessment of Cerenkov radiations and densitometric intensities confirmed that excision of BPDE-N^2-dG adducts was strongly affected by changes in the hydrogen bonding partner at the site of covalent modification. In particular, excision of (+)-*trans*-BPDE-N^2-dG was only moderately reduced when the complementary cytosine was replaced by adenine, but excision of the same BPDE-N^2-dG adduct in the *trans* configuration was reduced about 10-fold when the complementary deoxyribonucleotide was missing (Fig. 5B). On the other hand, (+)-*cis*-BPDE-N^2-dG was excised about 10-fold faster when located opposite cytosine than opposite adenine and, unexpectedly, the same (+)-*cis*-BPDE-N^2-dG was excised about 100-fold more efficiently in the presence of the complementary cytosine than in its absence (Fig. 5B). These remarkable differences prompted us to extend our analysis to substrates in which the (−)-*cis*-BPDE-N^2-dG isomer was located opposite adenine or a deletion site. In both cases, we observed strong inhibitory effects comparable to those found with the (+)-*cis*-BPDE-N^2-dG adduct (Fig. 5B).

Coincubation of substrate DNA with BPDE-modified deletion fragments. The lack of detectable carcinogen excision from deletion duplexes containing the BPDE adduct opposite a missing deoxyribonucleotide led us to perform competition experiments in which an excision repair substrate consisting of (−)-*cis*-BPDE-N^2-dG within the fully complementary sequence was combined with excess amounts of such deletion fragments. For example, 5 fmol of the radiolabeled substrate in the normal sequence was mixed with either 15 or 45 fmol of 139-mer fragments containing the (+)-*cis*-BPDE-N^2-dG adduct opposite a single dC deletion, and the mixtures were incubated in HeLa cell extract for 40 min. In these coincubation reactions, excision repair of the substrate was reduced to 38.0% of the control activity in the presence of a threefold molar excess of BPDE-modified deletion fragments. Furthermore, excision repair activity was reduced to 25.1% of the control level when a ninefold molar excess of the same deletion duplexes was added to the reactions (mean values of two independent experiments). In contrast, coincubation of the radiolabeled substrate with a three- or ninefold molar excess of unmodified control duplexes in the complementary sequence resulted in only marginal reduction of excision repair activity (to 90.2 and 97.3% of the control value, respectively). Collectively, these results indicate that (+)-*cis*-BPDE-N^2-dG adducts situated opposite deoxyribonucleotide deletion sites, although not repaired, are able to suppress excision of carcinogen-DNA adducts in HeLa cell extract by competing for nucleotide excision repair factors.

DISCUSSION

Conformation-dependent excision of carcinogen-DNA adducts. To identify molecular determinants of excision efficiency, human nucleotide excision repair was challenged with a series of structurally highly defined carcinogen-DNA lesions. First, we exploited the stereochemistry of BPDE-N^2-dG adducts to generate DNA substrates with distinctly different conformational properties and found that BPDE-N^2-dG adducts are processed by human nucleotide excision repair about 1 order of magnitude less efficiently in the (+)-*trans* or (−)-*trans* configurations than in the (+)-*cis* or (−)-*cis* configurations (Fig. 3 and 4). The structure of these DNA substrates was further modulated by changing deoxyribonucleotide composition opposite BPDE-N^2-dG lesions. Excision of both (+)-*cis*- and (−)-*cis*-BPDE-N^2-dG was reduced about 10-fold by a cytosine-to-adenine replacement in the complementary strand

opposite the modified guanine (Fig. 5), and excision of (+)-*trans*-, (+)-*cis*-, and (−)-*cis*-BPDE-N^2-dG was essentially suppressed when the partner deoxyribonucleotide opposite the lesion site was entirely missing (Fig. 5). Thus, a set of chemically identical but conformationally distinct BPDE-damaged substrates induced an unexpected range of human nucleotide excision repair activities with over-100-fold differences in the rates of damage excision. Collectively, these results show that human nucleotide excision repair efficiency is highly sensitive to the particular base pairing conformation arising at sites of damage.

Targeting of human nucleotide excision repair activity to sites of base pair displacement. Previous NMR analysis of BPDE-N^2-dG stereoisomers revealed two distinct structural motifs. In the 5′-TCGCT-3′ sequence context examined, (+)-*cis*-BPDE-N^2-dG involves intrahelical insertion of the benzo[*a*]pyrene moiety and local disruption of base pairing interactions. The modified guanine is displaced towards the minor groove and its cytosine partner is in the major groove (8). Intrahelical insertion of the benzo[*a*]pyrene residue is also a major structural feature of (−)-*cis*-BPDE-N^2-dG, but in this case, the modified guanine and its cytosine partner are both displaced in the direction of the major groove (11). In the two *trans*-BPDE-N^2-dG adducts, the BPDE residues are positioned in somewhat widened minor grooves and Watson-Crick hydrogen bonding is maintained at all base pairs (7, 12), although with reduced stability at the modified G · C base pair (56). Importantly, these profound differences in the NMR solution structures of DNA duplexes containing BPDE-N^2-dG adducts in the *cis* or *trans* configuration are paralleled by their distinctly different UV absorption and fluorescence characteristics (17). Combined with such detailed structural information, the 10-fold-higher excision repair rate stimulated by (+)-*cis*- and (−)-*cis*-BPDE-N^2-dG adducts relative to the chemically identical (+)-*trans* or (−)-*trans* isomers indicates that, in the human system, efficient nucleotide excision repair of BPDE-modified substrates is dependent on the degree of local base displacement at the lesion site. Interestingly, a distinctly different hierarchy of excision, with (+)-*cis*- and (+)-*trans*-BPDE-N^2-dG being processed more efficiently than the corresponding (−) isomers, was observed when (A)BC excinuclease (the prokaryotic nucleotide excision repair system) was tested with the same conformationally defined adducts in an identical sequence context (58). As noted before (24, 26, 34), these differences in the hierarchy of damage excision by prokaryotic and eukaryotic nucleotide excision repair systems possibly reflect diverging mechanisms of substrate discrimination.

The targeting of human nucleotide excision repair activity to displaced bases is supported by a recent comparison between the four BPDE-N^2-dG lesions of this study and a (−)-*trans*-BPDE-N^6-dA adduct that had been placed in codon 61 of the human *N-ras* sequence. This adenine adduct of BPDE provides a distinct structural theme characterized by intercalative carcinogen insertion without displacement of the modified base pair, although the respective hydrogen bonds are destabilized more severely than in the *trans*-BPDE-N^2-dG counterparts (57). Presumably because of these gradual differences in the extent of base pair disruption, the (−)-*trans*-BPDE-N^6-dA adduct in the *N-ras* codon 61 sequence is excised in vitro at a slightly faster rate than the *trans*-BPDE-N^2-dG adducts tested in this study. Consistent with the absence of stable extrahelical base displacement, however, this particular (−)-*trans*-BPDE-N^6-dA adduct is excised about six times more slowly than the two *cis*-BPDE-N^2-dG isomers (22). Targeting of excision repair activity to displaced bases is also consistent with previous studies from one of our laboratories, in which we demonstrated that disruption of proper base pairing is an essential determinant of DNA damage recognition by human nucleotide excision repair enzymes (19, 24).

Unexpectedly, excision activity was nearly abolished by removal of the cytosine partner in the complementary strand opposite the lesion. Upon NMR analysis (9, 10), the absence of a single deoxyribonucleotide opposite either (+)-*trans*- or (+)-*cis*-BPDE-N^2-dG has been shown to generate wedge-shaped intercalation complexes in which the modified guanine residues are displaced into the major and the minor grooves, respectively. However, these rather distorted duplexes are processed poorly by human nucleotide excision repair, indicating that a single base displaced into the major or minor groove is not as effective as the displacement of both bases for efficient excision. In competition experiments, we observed that (+)-*cis*-BPDE-N^2-dG adducts located opposite deletion sites suppress excision repair activity of appropriate substrates, suggesting that at least certain nucleotide excision repair factors interact with such BPDE-modified deletion duplexes but the resulting protein-DNA complexes fail to stimulate damage excision. Thus, the complementary undamaged base may have an unexpected and critical role in the assembly of functional incision complexes at sites of DNA damage. On the other hand, the structural consequences of dC→dA changes opposite BPDE-N^2-dG adducts are not completely understood. A characteristic shift in the light absorption spectra of BPDE-modified substrates led Pontén et al. (39) to conclude that the benzo[*a*]pyrene moiety may interact preferentially with adenine and, hence, promote incorporation of this purine into the double helix. Thus, adenine residues located across certain BPDE-N^2-dG adducts appear to exhibit less base displacement than cytosine and, in the cases of the helix-inserted (+)-*cis* and (−)-*cis* isomers, this observation correlates with 10-fold-lower levels of excision repair activity. Conversely, our study indicates that conformational distortions other than base pair displacement play a less important role as primary determinants of excision efficiency. For example, (+)-*trans*-BPDE-N^2-dG is only a moderate substrate for human nucleotide excision repair despite its more prominent ability to bend and unwind DNA (54, 55). Similarly, deletion-site substrates containing BPDE-guanine lesions are extremely inefficient substrates of human nucleotide excision repair despite their wedge-shaped helical distortions (9, 10).

Excision repair heterogeneity. The structure-activity relationship established in this study indicates preferential targeting of human nucleotide excision repair to BPDE-induced DNA distortions that displace both the modified base and its complementary partner. This finding provides a molecular frame for understanding and predicting the highly variable efficiency with which DNA adducts are excised from human genes (48, 49). It has been shown that carcinogen-DNA lesions are subject to strong sequence-dependent conformational polymorphisms. For example, in the 5′-TCGCT-3′ sequence context of this study (+)-*trans*-BPDE-N^2-dG induces a structural motif characterized by Watson-Crick base pairing (7) but a single nucleotide change on the 5′ side of the same lesion is associated with the appearance of an additional conformer (13). Similarly, acetylaminofluorene-C^8-dG adducts have been associated with sequence-specific polymorphisms in the extent of base pair denaturation (15, 18, 38, 45), and these variations constitute an important source of repair heterogeneity (34). Our results indicate that site-specific conformational differences affecting the local base pairing geometry may potentially result in excision rates that vary by more than 1 order of magnitude.

Excision from mutagenic intermediates generated by DNA replication. The replicative bypass of BPDE-N^2-dG-damaged DNA templates is often facilitated by insertion of adenines across modified guanines or by misalignment frameshift intermediates that generate deletion sites (33, 43). We observed that (+)-*trans*-, (+)-*cis*-, or (−)-*cis*-BPDE-N^2-dG adducts in substrates with a dA inserted opposite the modified guanines, or with a missing dC opposite these lesions, are excised less efficiently than they are from normal, fully complementary sequences. Most strikingly, excision of (+)-*cis*-BPDE-N^2-dG was reduced about 100-fold when the complementary deoxyribonucleotide was deleted. This ability to discriminate against duplex molecules containing a deoxyribonucleotide deletion site opposite DNA adducts appears to extend to a broad range of lesions, as we were able to observe the same response in the presence of other modifications that normally constitute efficient substrates for human nucleotide excision repair, i.e., acetylaminofluorene-C^8-dG adducts and a synthetic pivaloyldeoxyribose adduct (22).

Our present findings contrast with previous reports that have shown increased nucleotide excision repair activity in the same HeLa cell extract when bulky DNA adducts were combined with single G · T mismatches (32, 36). These studies proposed that, in some cases, efficient repair of mutagenic duplexes resulting from low-fidelity mechanisms of DNA replication would promote the fixation of a nucleotide change in both DNA strands (32, 36). Conversely, our present results indicate that mammalian cells possess a substrate discrimination strategy that minimizes excision of carcinogen-DNA adducts from certain mutagenic postreplication duplexes, particularly from those mutagenic intermediates that contain frameshift deletions opposite the lesion. This strategy reduces the contribution of DNA excision repair on the overall level of frameshift mutagenesis.

ACKNOWLEDGMENTS

We thank Claudia Rhiner for technical assistance and one of the referees for suggesting the coincubation experiment.

This work was supported by grant 3100-050518.97 from the Schweizerischer Nationalfonds zur Förderung der wissenschaftlichen Forschung to H.N. and by NIH grant CA-20851 and DOE grant DE-FGO2-88ER60405 to N.E.G.

REFERENCES

1. **Aboussekhra, A., M. Biggerstaff, M. K. K. Shivji, J. A. Vilpo, V. Moncollin, V. N. Podust, M. Protic, U. Hübscher, J.-M. Egly, and R. D. Wood.** 1995. Mammalian DNA nucleotide excision repair reconstituted with purified components. Cell **80:**859–868.
2. **Bohr, V. A., C. A. Smith, D. S. Okumoto, and P. C. Hanawalt.** 1985. DNA repair in an active gene: removal of pyrimidine dimers from the *DHFR* gene of CHO cells is much more efficient than in the genome overall. Cell **40:** 359–369.
3. **Chen, R.-H., V. M. Maher, J. Brouwer, P. van de Putte, and J. J. McCormick.** 1992. Preferential repair and strand-specific repair of benzo[*a*]pyrene diol epoxide adducts in the *HPRT* gene of diploid human fibroblasts. Proc. Natl. Acad. Sci. USA **89:**5413–5417.
4. **Cheng, S. C., B. D. Hilton, J. M. Roman, and A. Dipple.** 1989. DNA adducts from carcinogenic and noncarcinogenic enantiomers of benzo[*a*]pyrene dihydrodiol epoxide. Chem. Res. Toxicol. **2:**334–340.
5. **Conney, A. H.** 1982. Induction of microsomal enzymes by foreign chemicals and carcinogenesis by polycyclic aromatic hydrocarbons. Cancer Res. **42:** 4875–4917.
6. **Cosman, M., V. Ibanez, N. E. Geacintov, and R. G. Harvey.** 1990. Preparation and isolation of adducts in high yield derived from the binding of two benzo[*a*]pyrene-7,8-dihydroxy-9,10-oxide stereoisomers to the oligonucleotide d(ATATGTATA). Carcinogenesis **11:**1667–1672.
7. **Cosman, M., C. de los Santos, R. Fiala, B. E. Hingerty, S. B. Singh, V. Ibanez, L. A. Margulis, D. Live, N. E. Geacintov, S. Broyde, and D. J. Patel.** 1992. Solution conformation of the major adduct between the carcinogen (+)-*anti*-benzo[*a*]pyrene diol epoxide and DNA. Proc. Natl. Acad. Sci. USA **89:**1914–1918.
8. **Cosman, M., C. de los Santos, R. Fiala, B. E. Hingerty, V. Ibanez, E. Luna, R. G. Harvey, N. E. Geacintov, S. Broyde, and D. J. Patel.** 1993. Solution conformation of the (+)-*cis-anti*-[BP]dG adduct in a DNA duplex: intercalation of the covalently attached benzo[*a*]pyrenyl ring into the helix and displacement of the modified deoxyguanosine. Biochemistry **32:**4145–4155.
9. **Cosman, M., R. Fiala, B. E. Hingerty, S. Amin, N. E. Geacintov, S. Broyde, and D. J. Patel.** 1994. Solution conformation of the (+)-*trans-anti*-[BP]dG adduct opposite a deletion site in a DNA duplex: intercalation of the covalently attached benzo[*a*]pyrene in the helix with base displacement of the modified deoxyguanosine into the major groove. Biochemistry **33:**11507–11517.
10. **Cosman, M., R. Fiala, B. E. Hingerty, S. Amin, N. E. Geacintov, S. Broyde, and D. J. Patel.** 1994. Solution conformation of the (+)-*cis-anti*-[BP]dG adduct opposite a deletion site in a DNA duplex: intercalation of the covalently attached benzo[*a*]pyrene in the helix with base displacement of the modified deoxyguanosine into the minor groove. Biochemistry **33:**11518–11527.
11. **Cosman, M., B. E. Hingerty, N. Luneva, S. Amin, N. E. Geacintov, S. Broyde, and D. J. Patel.** 1996. Solution conformation of the (−)-*cis-anti*-benzo[*a*]pyrenyl-dG adduct opposite dC in a DNA duplex: intercalation of the covalently attached BP ring into the helix with base displacement of the modified deoxyguanosine into the major groove. Biochemistry **35:**9850–9863.
12. **de los Santos, C., M. Cosman, B. E. Hingerty, V. Ibanez, L. A. Margulis, N. E. Geacintov, S. Broyde, and D. J. Patel.** 1992. Influence of benzo[*a*]pyrene diol epoxide chirality on solution conformations of DNA covalent adducts: the (−)-*trans-anti*-[BP]G · C adduct structure and comparison with the (+)-*trans-anti*-[BP]G · C enantiomer. Biochemistry **31:**5245–5252.
13. **Fountain, M. A., and T. R. Krugh.** 1995. Structural characterization of a (+)-*trans-anti*-benzo[*a*]pyrene-DNA adduct using NMR, restrained energy minimization, and molecular dynamics. Biochemistry **34:**3152–3161.
14. **Friedberg, E. C., G. C. Walker, and W. Siede.** 1995. DNA repair and mutagenesis. American Society for Microbiology, Washington, D.C.
15. **Fuchs, R. P. P., and M. Daune.** 1971. Physical studies on deoxyribonucleic acid after covalent binding of a carcinogen. Biochemistry **11:**2659–2666.
16. **Gao, S., R. Drouin, and G. P. Holmquist.** 1994. DNA repair rates mapped along the human *PGK1* gene at nucleotide resolution. Science **263:**1438–1440.
17. **Geacintov, N. E., M. Cosman, B. Mao, A. Alfano, V. Ibanez, and R. G. Harvey.** 1991. Spectroscopic characteristics and site I/II classification of *cis* and *trans* benzo[*a*]pyrene diol epoxide enantiomer-guanosine adducts in oligonucleotides and polynucleotides. Carcinogenesis **12:**2099–2108.
18. **Grunberger, D., J. H. Nelson, C. R. Cantor, and I. B. Weinstein.** 1970. Coding and conformational properties of oligonucleotides modified with the carcinogen N-2-acetylaminofluorene. Proc. Natl. Acad. Sci. USA **66:**488–494.
19. **Gunz, D., M. T. Hess, and H. Naegeli.** 1996. Recognition of DNA adducts by human nucleotide excision repair. J. Biol. Chem. **271:**25089–25098.
20. **Hanawalt, P. C.** 1994. Transcription-coupled repair and human diseases. Science **266:**1957–1958.
21. **Hansson, J., M. Munn, W. D. Rupp, R. Kahn, and R. D. Wood.** 1989. Localization of DNA repair synthesis by human cell extracts to a short region at the site of a lesion. J. Biol. Chem. **264:**21788–21792.
22. **Hess, M. T., N. E. Geacintov, and H. Naegeli.** Unpublished data.
23. **Hess, M. T., U. Schwitter, M. Petretta, B. Giese, and H. Naegeli.** 1996. Site-specific DNA substrates for human excision repair: comparison between deoxyribose and base adducts. Chem. Biol. **3:**121–128.
24. **Hess, M. T., U. Schwitter, M. Petretta, B. Giese, and H. Naegeli.** 1997. Bipartite substrate discrimination by human nucleotide excision repair. Proc. Natl. Acad. Sci. USA **94:**6664–6669.
25. **Huang, J.-C., D. Svoboda, J. T. Reardon, and A. Sancar.** 1992. Human nucleotide excision nuclease removes thymine dimers from DNA by incising the 22nd phosphodiester bond 5′ and the 6th phosphodiester bond 3′ to the photodimer. Proc. Natl. Acad. Sci. USA **89:**3664–3668.
26. **Huang, J.-C., D. S. Hsu, A. Kazantsev, and A. Sancar.** 1994. Substrate spectrum of human excinuclease: repair of abasic sites, methylated bases, mismatches, and bulky adducts. Proc. Natl. Acad. Sci. USA **91:**12213–12217.
27. **Manley, J. L., A. Fire, A. Cano, P. A. Sharp, and M. L. Gefter.** 1980. DNA-dependent transcription of adenovirus genes in a soluble whole-cell extract. Proc. Natl. Acad. Sci. USA **77:**3855–3859.
28. **Matsunaga, T., D. Mu, C.-H. Park, J. T. Reardon, and A. Sancar.** 1995. Human DNA repair excision nuclease. J. Biol. Chem. **270:**20862–20869.
29. **Mellon, I., G. Spivak, and P. C. Hanawalt.** 1987. Selective removal of transcription-blocking DNA damage from the transcribed strand of the mammalian DHFR gene. Cell **51:**241–249.
30. **Mitchell, D. L., and R. S. Nairn.** 1989. The biology of the (6-4) photoproduct. Photochem. Photobiol. **49:**805–819.
31. **Moggs, J. G., K. J. Yarema, J. M. Essigmann, and R. D. Wood.** 1996. Analysis of incision sites produced by human cell extracts and purified proteins during nucleotide excision repair of a 1,3-intrastrand d(GpTpG)-cisplatin adduct. J. Biol. Chem. **271:**7177–7186.
32. **Moggs, J. G., D. E. Szymkowski, M. Yamada, P. Karran, and R. D. Wood.** 1997. Differential human nucleotide excision repair of paired and mispaired

cisplatin-DNA adducts. Nucleic Acids Res. **25:**480–490.
33. **Moriya, M., S. Spiegel, A. Fernandes, S. Amin, T. Liu, N. E. Geacintov, and A. P. Grollman.** 1996. Fidelity of translesional synthesis past benzo[*a*]pyrene diol epoxide-2′-deoxyguanosine DNA adducts: marked effects of host cell, sequence context, and chirality. Biochemistry **35:**16646–16651.
34. **Mu, D., E. Bertrand-Burggraf, J. J. Huang, R. P. P. Fuchs, and A. Sancar.** 1994. Human and *E. coli* excinucleases are affected differently by the sequence context of acetylaminofluorene-guanine adduct. Nucleic Acids Res. **22:**4869–4871.
35. **Mu, D., D. S. Hsu, and A. Sancar.** 1996. Reaction mechanism of human DNA repair excision nuclease. J. Biol. Chem. **271:**8285–8294.
36. **Mu, D., M. Tursun, D. R. Duckett, J. T. Drummond, P. Modrich, and A. Sancar.** 1997. Recognition and repair of compound DNA lesions (base damage and mismatch) by human mismatch repair and excision repair systems. Mol. Cell. Biol. **17:**760–769.
37. **Naegeli, H.** 1997. Mechanisms of DNA damage recognition in mammalian cells. R. G. Landes, Austin, Tex.
38. **O'Handley, S. F., D. G. Sanford, R. Xu, C. C. Lester, B. E. Hingerty, S. Broyde, and T. R. Krugh.** 1993. Structural characterization of an N-acetyl-2-aminofluorene (AAF) modified DNA oligomer by NMR, energy minimization, and molecular dynamics. Biochemistry **32:**2481–2497.
39. **Pontén, I., S. K. Kim, A. Gräslund, B. Nordén, and B. Jernström.** 1994. Synthesis and characterization of a (+)-anti-benzo[*a*]pyrene 7,8-dihydrodiol 9,10-epoxide-oligonucleotide adduct, p. 433–436. *In* K. Hemminki, D. E. G. Dipple, F. F. Shuker, D. Kadlubar, D. Segerbäck, and H. Bartsch (ed.), DNA adducts: identification and biological significance. International Agency for Research on Cancer scientific publication no. 125. International Agency for Research on Cancer, Lyon, France.
40. **Reardon, J. T., L. H. Thompson, and A. Sancar.** 1997. Rodent UV-sensitive mutant cell lines in complementation groups 6-10 have normal general excision repair activity. Nucleic Acids Res. **25:**1015–1021.
41. **Ruggieri, B., M. DiRado, S. Y. Zhang, B. Bauer, T. Goodrow, and A. J. P. Klein-Szanto.** 1993. Benzo[*a*]pyrene-induced murine skin tumors exhibit frequent and characteristic G to T mutations in the *p53* gene. Proc. Natl. Acad. Sci. USA **90:**1013–1017.
42. **Sancar, A.** 1996. DNA excision repair. Annu. Rev. Biochem. **65:**43–81.
43. **Shibutani, S., L. A. Margulis, N. E. Geacintov, and A. P. Grollman.** 1993. Translesional synthesis on a DNA template containing single stereoisomers of dG-(+)- or dG-(−)-*anti*-BPDE (7,8-dihydroxy-*anti*-9,10-epoxy-7,8,9,10-tetrahydrobenzo[*a*]pyrene). Biochemistry **32:**7531–7541.
44. **Tornaletti, S., and G. P. Pfeifer.** 1994. Slow repair of pyrimidine dimers at *p53* mutation hotspots in skin cancer. Science **263:**1436–1438.
45. **Veaute, X., and R. P. P. Fuchs.** 1991. Polymorphism in N-2-acetylaminofluorene induced DNA structure as revealed by DNase I footprinting. Nucleic Acids Res. **19:**5603–5606.
46. **Venema, J., Z. Bartosová, A. T. Natarajan, A. A. van Zeeland, and L. H. F. Mullenders.** 1992. Transcription affects the rate but not the extent of repair of cyclobutane pyrimidine dimers in the human adenosine deaminase gene. J. Biol. Chem. **267:**8852–8856.
47. **Vousden, K. H., J. L. Bos, C. J. Marshall, and D. H. Phillips.** 1986. Mutations activating human c-Ha-*ras1* protooncogene (*HRAS1*) induced by chemical carcinogens and depurination. Proc. Natl. Acad. Sci. USA **83:**1222–1226.
48. **Wei, D., V. M. Maher, and J. J. McCormick.** 1995. Site-specific rates of excision repair of benzo[*a*]pyrene diol epoxide adducts in the hypoxanthine phophoribosyltransferase gene of human fibroblasts: correlation with mutation spectra. Proc. Natl. Acad. Sci. USA **92:**2204–2208.
49. **Wei, D., V. M. Maher, and J. J. McCormick.** 1996. Site-specific excision repair of 1-nitrosopyrene-induced DNA adducts at the nucleotide level in the *HPRT* gene of human fibroblasts: effect of adduct conformation on the pattern of site-specific repair. Mol. Cell. Biol. **16:**3714–3719.
50. **Wei, S.-J. C., R. L. Chang, E. Hennig, X. X. Cui, K. A. Merkler, C.-Q. Wong, H. Yagi, and A. H. Conney.** 1994. Mutagenic selectivity at the *HPRT* locus in V-79 cells: comparison of mutations caused by bay-region benzo[*a*]pyrene 7,8-9,10-epoxide enantiomers with high and low carcinogenic activity. Carcinogenesis **15:**1729–1735.
51. **Wood, R. D., P. Robins, and T. Lindahl.** 1988. Complementation of the xeroderma pigmentosum DNA repair defect in cell-free extracts. Cell **53:**97–106.
52. **Wood, R. D.** 1996. DNA repair in eukaryotes. Annu. Rev. Biochem. **65:**135–167.
53. **Xu, R., S. Amin, and N. E. Geacintov.** Unpublished data.
54. **Xu, R., S. Birke, S. E. Carberry, N. E. Geacintov, C. E. Swenberg, and R. G. Harvey.** 1992. Differences in unwinding of supercoiled DNA induced by the two enantiomers of *anti*-benzo[*a*]pyrene diol epoxide. Nucleic Acids Res. **20:**6167–6176.
55. **Xu, R., B. Mao, J. Xu, B. Li, S. Birke, C. E. Swenberg, and N. E. Geacintov.** 1995. Stereochemistry-dependent bending in oligonucleotide duplexes induced by site-specific covalent benzo[*a*]pyrene diol epoxide-guanine lesions. Nucleic Acids Res. **23:**2314–2319.
56. **Ya, N.-Q., S. Smirnov, M. Cosman, S. Bhanot, V. Ibanez, and N. E. Geacintov.** 1994. Thermal stabilities of benzo[*a*]pyrene diol epoxide-modified oligonucleotide duplexes. Effects of mismatched complementary strands and bulges, p. 349–366. *In* R. H. Sarma and M. H. Sarma (ed.), Structural biology: the state of the art. Proceedings of the 8th conversation. Adenine Press, Schenectady, N.Y.
57. **Zegar, I. S., S. J. Kim, T. N. Johansen, P. J. Horton, C. M. Harris, T. M. Harris, and M. P. Stone.** 1996. Adduction of the human *N-ras* codon 61 sequence with (−)-(7*S*,8*R*,9*R*,10*S*)-7,8-dihydroxy-9,10-epoxy-7,8,9,10-tetrahydrobenzo[*a*]pyrene: structural refinement of the intercalated SRSR(61,2) (−)-(7*S*,8*R*,9*R*,10*S*)-N^6-[10-(7,8,9,10-tetrahydrobenzo[*a*]pyrenyl)]-2′-deoxyadenosyl adduct from ^{1}H NMR. Biochemistry **35:**6212–6224.
58. **Zou, Y., T. Liu, N. E. Geacintov, and B. Van Houten.** 1995. Interaction of the UvrABC nuclease with a DNA duplex containing a single stereoisomer of dG-(+)- or dG-(−)-*anti*-BPDE. Biochemistry **34:**13582–13593.